Journal of the European Ceramic Society 36 (2016) 147–153

Contents lists available at www.sciencedirect.com

Journal of the European Ceramic Society

journal homepage: www.elsevier.com/locate/jeurceramsoc

The influence of unshielded small cracks in the fracture toughness of yttria and of ceria stabilised zirconia

Latifa Melk[a,b,c], Miquel Turon-Vinas[a,b], Joan Josep Roa[a,b], Marta-Lena Antti[c], Marc Anglada[a,b,*]

[a] CIEFMA—Department of Materials Science and Metallurgical Engineering, ETSEIB, Universitat Politècnica de Catalunya, 08028 Barcelona, Spain
[b] CRnE, Campus Diagonal Sud, Edifici C', Universitat Politècnica de Catalunya, 08028 Barcelona, Spain
[c] Department of Engineering Sciences and Mathematics, Luleå University of Technology, 97187 Luleå, Sweden

ARTICLE INFO

Article history:
Received 24 August 2015
Accepted 13 September 2015
Available online 26 September 2015

Keywords:
Fracture resistance curves
Fracture stress
Zirconia
3Y–ZrO_2
12Ce–ZrO_2

ABSTRACT

The fracture toughness, K_{IC} of two 3Y–ZrO_2 with different grain size (177 and 330 nm) and 12Ce–ZrO_2 were determined from a sharp micro-machined notch by Ultra-Short Pulsed Laser Ablation (UPLA) where a micro-cracked zone and non-transformed is generated in front of the notch. The notch plus the damage behaved as an unshielded edge surface crack. The fracture stress, σ_f of both 330 nm-3Y–ZrO_2 and 12Ce–ZrO_2 with similar short crack sizes were found to be comparable in despite of their different published *R*-curves. The results of K_{IC} were discussed in terms of the type of cracks induced and by using a simple *R*-curve model. It was concluded that for the development of high strength composites with 12Ce–ZrO_2 as the matrix, the relevant K_{IC} that controls the σ_f with surface unshielded short cracks is much closer to the intrinsic K_{IC} than to the indentation K_{IC} or to the plateau K_{IC} of long cracks.

1. Introduction

Fracture in advanced ceramics is caused by flaws with variable dimensions, generally of several tens of micrometers. In principle, it is possible to predict their fracture stress, σ_f, from fracture mechanics if the critical natural flaw and the fracture toughness, K_{IC}, are precisely determined. However, an accurate prediction requires a specific knowledge of the shape of the critical flaw, which is difficult to be precisely modeled as a two dimensional crack.

Regarding the actual K_{IC} of zirconia ceramics with phase transformation toughening, K_{IC} is characterized by a fracture resistance curve (K_R), which depends on crack length and which is also referred to as *R*-curve [1]. The *R*-curve is usually known for long cracks of several millimeters in length. It is often obtained from fracture testing prismatic specimens by the single edge V-notch beam (SEVNB) method.

Nowadays, one of the zirconia ceramics widely used in biomedical applications is zirconia doped with 3 mol.% of yttria known as 3Y–ZrO_2. It has a high strength (>1000 MPa), but only a moderate K_{IC} (4–5 MPa$\sqrt{m}$) and it suffers from slow subcritical crack growth and low temperature degradation (LTD) after exposure to humid environments [2]. One possible way to increase the K_{IC} and the resistance to LTD is to develop new composites in which the matrix of zirconia is doped with ceria and the reinforcement is a harder phase such as alumina [3]. Although subcritical crack growth is still present [4], zirconia doped with ceria is resistant to LTD and it has a large transformability under stress, as measured by indentation methods, and a high plateau in the *R*-curve for ceria concentrations in the range of 9–12 mol.% [4–6]. However, when cracks are of dimensions similar to natural cracks, it is not obvious to which extend the *R*-curve and the crack size could determine the strength [7].

If the flaw population size and the transformation stress both decrease, then fracture may be controlled by phase transformation and it can be flaw independent in the very small flaw range. As the size of the critical flaw and transformation stress increase, fracture is controlled by the flaw size and the *R*-curve. There are experimental results from literature showing that natural small cracks tend to have lower *R*-curves [7].

The objective of the present work is to investigate the influence of transformation toughening on the σ_f and on the K_{IC} of 12Ce–ZrO_2 and 3Y–ZrO_2 with similar small two dimensional artificial surface cracks of dimensions as close as possible to natural cracks. For this purpose, we have machined very shallow single edge notches by a novel method using Ultra-short Pulsed Laser Ablation (UPLA) on the surface of rectangular bending bars on two 3Y–ZrO_2 with different

* Corresponding author at: CIEFMA—Department of Materials Science and Metallurgical Engineering, ETSEIB, Universitat Politècnica de Catalunya, 08028 Barcelona, Spain.
E-mail address: marc.j.anglada@upc.edu (M. Anglada).

http://dx.doi.org/10.1016/j.jeurceramsoc.2015.09.017
0955-2219/

grain size, and on 12Ce–ZrO_2. These two zirconia ceramics have *R*-curves with completely different plateau levels and steepness. The σ_f and the K_{IC} are measured from a similar small crack induced in each material, and they are discussed in terms of their published *R*-curves.

2. Experimental procedure

2.1. Preparation of specimens

Commercial powders of 3Y–ZrO_2 (ZrO_2 with 3 mol.% Y_2O_3) from Tosoh (gradeTZ-3YSB-E) and 12Ce–ZrO_2 (ZrO_2 with 12 mol.% CeO_2) from Daiichi Kigenso Kagaku Kogyo of Japan (grade CEZ-12SD) were cold and uniaxially pressed at 100 MPa in the form of bars ($3 \times 4 \times 50\,mm^3$), then sintered in an alumina tube furnace (model ST-18, Forns Hobersal S.L., Spain) at 1450 °C with heating and cooling rates of 3 °C/min and a holding time of 1 h and 2 h for 3Y–ZrO_2 and 12Ce–ZrO_2, respectively. Using the Archimedes' principle, the bulk materials result in a density of above 99.5% for 330 nm-3Y–ZrO_2 and 99% for 12Ce-TZP of the theoretical density. The specimens were polished following the standard grinding and polishing methods down to 3 μm.

Additional specimens of 3Y–ZrO_2 were prepared by Spark Plasma Sintering (SPS) (SPS FCT HP D25I, FCT System GmβH) with a finer grain size (177 nm), and in the present study they will be referred to as 177 nm-3Y–ZrO_2. The samples were sintered at maximum temperature of 1350 °C with heating and cooling rates of 100 °C/min and a holding time of 5 min. A pressure of 50 MPa was maintained during the sintering cycle. Further information on sintering details can be found elsewhere [8]. The final samples were ceramic discs with 3 mm thickness and 40 mm diameter cut into bars ($4 \times 2.5 \times 35\,mm^3$) with a density of 99.4% of the theoretical density.

The average grain size was determined by the conventional linear intercept method using a total of ten micrographs per specimen in order to have statistical significance. The micrographs were obtained by using a field emission scanning electron microscope (FESEM, JEOL 7001F).

2.2. The starting defect size

A single edge V-notch was produced by UPLA on the center of the surface of prismatic specimens perpendicularly to the 4 mm width. Laser pulses (120 fs, 795 nm) were induced by means of a commercial Ti:sapphire oscillator (Tsunami, Spectra Physics) and a regenerative amplifier system (Spitfire, Spectra Physics) based on chirped pulsed amplification. The pulses were linearly polarized and the repetition rate was 1 kHz. The pulse energy used was 5 μJ and the focusing system used was an achromatic doublet lens with focal length of 50 mm. The samples were placed on a XYZ motorized stage and moved along one of the horizontal axis with a scanning speed of 50 μm/s. Four passes were needed to achieve the desired notch depth. The shape of the final notch was similar to a V-notch and its depth was ranged between 24 and 30 μm.

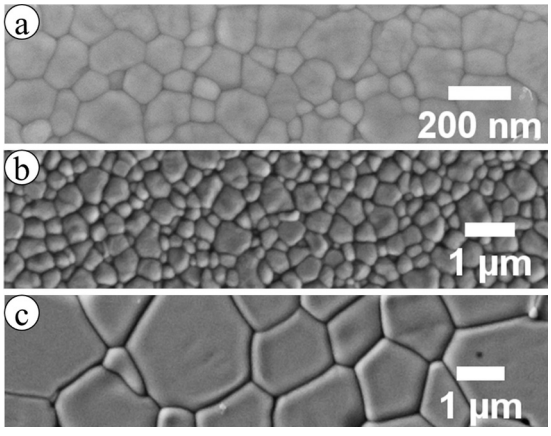

Fig. 1. FESEM micrographs showing the grain size of (a) 177 nm-3Y–ZrO2, (b) 330 nm-Y–ZrO2 and (c) 12Ce–ZrO2 after thermal etching.

Fracture surface analysis was done in a field emission scanning electron microscope (FESEM). The damage induced by UPLA below the surface was characterized using a dual beam focused ion beam (FIB)/FESEM (Neon40, Carl Zeiss AG, Germany). A thin platinum layer was deposited on the sample prior to FIB machining in order to flatten the surface and minimize ion-beam damage and curtain effect. A Gallium ion (Ga^+) source was used to mill the surface at a voltage of 30 kV. The final polishing of the cross-sections was performed at 500 pA and the surface was observed by FESEM at regions around the notch.

Raman spectra were collected with a spectrometer Jobin-Yvon LabRam HR 800 coupled to an Olympus optical microscope BXFM with an objective of 50× and to a CCD detector (liquid nitrogen cooled). A laser wavelength of 532 nm was used as source of excitation. The spectrum integration time was 30 s, with averaging the recorded spectra over two successive measurements.

2.3. Strength and fracture toughness measurements

Finally, the single edge V-notched bar specimens were tested in a servohydraulic fatigue testing machine (model 8511, Instron, USA) using a four point bending test configuration with spans of 40/20 mm and under a high constant stress rate equal to 130 MPa s^{-1} in laboratory air. The number of specimens tested was 5 for the 330 nm-3Y–ZrO_2 samples. In the case of 177 nm-3Y–ZrO_2, the notched bar specimens were tested in a four point bending test device (DEBEN, Microtest, UK) in air with spans of 30/12 mm. The average stress rate was 2.4 MPa s^{-1}. The influence of strain rate on the σ_f of the cracked bars was studied in the case of 330 nm-3Y–ZrO_2 specimens. No significant effect of strain rate has been found when two additional specimens were tested at different strain rates by a factor of 50.

Three specimens were used for each composition, while only two specimens were used for the measurement of the σ_f of 12Ce–ZrO_2. The stress intensity factor (K_I) was obtained by using the following expression [9]:

$$K_I = \sigma Y \sqrt{a} \tag{1}$$

$$Y = \frac{1.1215\sqrt{\pi}}{\eta^{3/2}} \left[\frac{5}{8} - \frac{5}{12}\delta + \frac{1}{8}\delta^2\eta^6 + \frac{3}{8}\exp\left(-\frac{6.1342\delta}{\eta}\right) \right] \tag{2}$$

where σ_f is the maximum stress on the surface which is given by:

$$\sigma_f = \frac{3F(S_1 - S_2)}{2BW^2} \tag{3}$$

S_1 and S_2 are the outer and inner spans respectively, B is the thickness, W *is* the width, F *is* the applied load, a is the crack length, $\delta = a/W$, and $\eta = 1 - \delta$.

On the other hand, the residual imprint and the damage related to Vickers' indentation imprints were assessed by inspecting the indentations through confocal laser scanning microscopy (CLSM, LEXT OL3 100, Olympus). The response to contact loading by Vickers indentation was determined by calculating the indentation fracture toughness (K_{ind}) with the purpose of comparing with other studies. Hence, the equation of Anstis et al. [10] for median radial cracks was used since it has often been used in the literature independently of the shape of the cracks. K_{ind} was reported only for analysing the response to contact loading for comparative purposes, but it does